MWCNT/rGO/natural rubber latex dispersions for innovative, piezo-resistive and cement-based composite sensors

Letizia Verdolotti
National Research Council
Chiara Santillo
National Research Council
Gennaro Rollo
National Research Council
Giovanni Romanelli
Rutherford Appleton Laboratory
Marino Lavorgna (mlavorgn@unina.it)
National Research Council
Barbara Liguori
University of Naples Federico II
Giuseppe Lama
National Research Council
Enrico Preziosi
University of Rome Tor Vergata
Roberto Senesi
University of Rome Tor Vergata
Carla Andreani
University of Rome Tor Vergata
Marco Di Prisco
Politecnico di Milano, Department of Civil and Environmental Engineering

Research Article

Keywords: Strain sensors, mortar composites, MWCNT and rGO, piezoresistive properties

Posted Date: February 19th, 2021

DOI: https://doi.org/10.21203/rs.3.rs-234097/v1

Abstract

The present study is focused on the development and characterization of innovative cementitious-based composite sensors. In particular, multifunctional cement mortar composites with enhanced functional, piezo-resistive, properties are designed with Multiwall Carbon Nanotube-MWCNTs and reduced Graphene Oxide-rGO dispersed in a natural-rubber latex aqueous dispersion, by exploiting both the concept of confining of the conductive filler in the polymeric phase. The manufactured cement-based composites were characterized by means of Inelastic Neutron Scattering to assess the hydration reactions and the interactions of natural rubber with the hydrated cement phases and by Electron Scanning Microscopy and X-Ray diffraction to evaluate the morphological and mineralogical structure, respectively. Piezo-resistive properties to assess electro-mechanical behavior in strain condition are also measured. The results show that the presence of natural-rubber latex permits to obtain a three-dimensional rGO/MWCNTs segregate structure which catalyzes the formation of hydrated phases of the cement and increases the piezo-resistive sensitivity of mortar composites, representing a reliable approach in developing innovative mortar-based piezoresistive strain sensors.

Introduction

In the civil-construction sector, the new global-technological standards, requiring increasingly “smart” infrastructures, are guiding the development of building materials with “ultra-performing multifunctional characteristics”. In particular, research, development and innovativeness are addressing precisely towards the creation of innovative multifunctional construction materials (such as mortars and concretes) with improved mechanical properties as well as functional properties such as thermal insulation, electrical conductivity, photo-catalysis, etc, through the tailoring of the nanometer structure of the cementitious phase. In fact, since most of the mortar and concrete damages occur in cementitious-based binding materials, it is possible to improve them by tracing back to their chemical and mechanical defects, designing more effective micron and submicron structures by exploiting the potentials of nanoparticles [1-2].

In this respect, the development of cementitious-based composites by using carbonaceous filler (i.e. Multiwall Carbon Nanotubes (MWCNTs), Graphene and/or its derivatives) able to strengthen the nanostructure of cement hydrated phases, and enabling the obtainment of piezo-resistive strain sensors useful for the structural health monitoring of buildings, is a very topical issue and yet to be fully explored [3-5]. In particular, the enhancement of structural and functional properties of cement-based composites realizes when the nanometric filler is loaded at a defined concentration, i.e. percolation threshold which enables the formation of a continuous network throughout the cementitious matrix. The filler amount to get percolation depends on the geometrical properties of the filler (i.e. shape as 1-dimensional or 2-dimensional filler and aspect ratio) and, generally, the best improvements of structural and functional performances are observed for filler contents from 1wt% (with respect to the cement fraction) up to several percentage units [6-10]. Moreover, the peculiarities of cementitious-based composites strongly depend on the ability to homogeneously disperse carbonaceous filler within the mortar and concrete

volume, without destroying their integrity and avoiding marked aggregation/separation. Furthermore, to obtain an improvement in the mechanical and functional properties of the composite, it is required a good interaction at the carbonaceous filler-matrix interface (i.e. cement). Generally, the strong tendency of these fillers to agglomerate due to the presence of attractive forces (Van der Waals), can hinder the positive effect of the filler. In order to control the dispersion homogeneity of the carbonaceous fillers (carbon nanotubes (CNTs), graphene and its derivatives) into organic or inorganic matrices, various methods have been proposed including physical techniques, such as ultrasonication, ball milling and mechanical stirring, or chemical methods, such as the use of surfactants (able to improve the dispersion of filler in an aqueous solution by reducing the surface tension of water), covalent functionalization of fillers or a combination of these methods [5, 11-15]. As far as the composites with inorganic matrix are concerned, all these methods promote the dispersion of the carbonaceous filler in the whole binding phase generated from hydration of the cement, which being very large requires a huge filler content to get effective percolation, thus resulting in the costs/performance balance as a material with poor electrical properties or highly expensive.

Several approaches have been carried out in the recent decades on the use of carbonaceous fillers in order to promote the cement hydration as well as to improve the resulting structural, morphological and functional properties of cementitious-based systems [16]. In particular, Bai et al. [17] showed that the introduction of silica fume facilitating the graphene dispersion and increasing the interfacial strength between the filler and cement matrix enhances the compressive strength and electrical properties of the cement-based composite. Zhan et al. [9] synthesized CNTs in situ on the surface of fly ash (CNT-coated FA) and then these particles were incorporated into cement mortars. The composite with a 2 wt% of CNT-coated FA has good mechanical and piezoresistive properties. Some research also used a mixture of carbonaceous filler for the development of mortar-composites. For example, Han et al. [10] added both CNTs and carbon black (NCB) into cement mortar enhancing their electrical conductivity and endowing them of stable and sensitive piezoresistivity.

Recently, some of the authors have developed an innovative approach to prepare effective carbonaceous-based composite materials. This method involves the distribution of the filler in an aqueous-rubber latex dispersion. The filler, both carbon nanotubes and graphene derivatives, is assembled on the surface of the latex particles, avoiding aggregation and realizing a three-dimensional network with the fillers localized only in between the interstices of the single latex particles which randomly coalesce to produce a continuous rubbery phase [18]. This approach is very effective and allows to reducing the amount of filler needed to reach a percolating-network into the polymeric matrix (as compared to the amount for the geometrical percolation). [19] This concept can be translated to the cement-based composite materials, in order to promote the distribution of the conductive filler wherein the rubber latex coalesces, allowing the percolation with filler amounts lower than those needed when the filler is randomly dispersed throughout the cement-based hydrated phase.

Despite the huge efforts addressed to investigate the realization of cementitious composites with carbonaceous fillers, few are the scientific papers focused on the understanding of peculiar role of the

carbonaceous fillers in the chemical hydration processes of cement (micro and nanostructure of CSH) and in the mechanisms of mechanical improvement and exploitation of functional properties [20, 21].

Insights about the physical and chemical properties of hydrated cement can be achieved by means of Inelastic Neutron Scattering (INS)[22, 23]. INS is an experimental technique probing lattice, inter- and intramolecular vibrations in condensed matter systems [24], similarly to infra-red and Raman spectroscopies [25-27], yet without selection rules. Experimental spectra display a dominant scattering contribution from hydrogen, in the so-called incoherent approximation [28], making INS an exquisite technique to capture lattice modes in molecular systems, such as water and latex. As neutron scattering is particularly sensitive to hydrogen, as opposed to photon-based techniques where the signal is proportional to the atomic number, INS provides an important complementary information to vibrational techniques such as Raman and infra-red spectroscopies (see e.g., [29]). Moreover, owing to the high penetration depth achieved in neutron experiments, INS can be applied to real-size and bulk materials, still providing a description of the system at the atomic scale. Over the last decades, INS investigations have tackled the hydration mechanism in traditional cements by probing the creation of Ca-OH bonds [30], and the hydration mechanism and water dynamics in concrete [31] and isolated cement components [32, 33]. However, investigations through INS on cementitious-based composite with carbonaceous filler are still missing.

Starting from this background, cementitious-based composites modified with carbonaceous fillers previously assembled on rubber latex particles, were prepared through a multi-steps approach:

(a) selection of the suitable carbonaceous-filler (Multiwall Carbon Nanotubes-MWCNT, graphene-derivatives and a mixture of them) and the dispersion media (rubber-based latex dispersion);

(b) mix design of the cementitious-based composite formulation by selecting the amount of filler and other components, such as cement, water, and additives;

(c) assembling of reduced graphene oxide and MWCNT particles onto the latex particles through a tailored chemical reduction and mixing and workability of the resulting cementitious-based mixture.

The produced cementitious-based composites (namely mortar composites MC) containing the carbonaceous fillers, were characterized by means of INS to evaluate the chemical hydration of anhydrous cementitious phases, Scanning Electron Microscopy (SEM) and X-Ray diffraction to evaluate, respectively, the morphological and mineralogical structure and piezo-resistive properties to assess electro-mechanical properties in strain condition.

Results And Discussion

Chemical characterization by Inelastic Neutron Scattering-INS

Figure 1 shows the INS spectra of M_0, M_1, CM_2 and CM_3 mortar composites after subtraction of the backgrounds from dry cement and empty container. As the main contribution to the spectra comes from hydrogen atoms involved in cement hydration, data were compared with a deionised H_2O sample measured at the same temperature, also shown in Figure 1. From the bulk-H_2O spectrum, it is possible to recognize the translational (below 400 cm^{-1}) and vibrational (around 600 cm^{-1}) modes arising from the intermolecular interactions and the hydrogen-bonding network. By comparison, it is noticed how the sharp vibrational feature in bulk H_2O is clearly broadened and red-shifted in the mortar samples, as a consequence of the different interactions that coordinated water molecules experience within the mortar structure. The overall shift of the vibrational bands to lower frequencies corresponds to a picture whereby some H_2O molecules undergo rotations that are less hindered than in the bulk, due to the breaking of the hydrogen-bonding network. At lower energies, the sharp translational features in bulk water at 50 cm^{-1}, 220 cm^{-1}, and 305 cm^{-1} disappear, replaced by more complex lattice and translational motions between 70 cm^{-1} and 400 cm^{-1} in the hydrated cements, resulting from the coordination of water to the cement, as well as the creation of new Calcium Silicate Hydrated species. In particular, the strong peak at ca. 330 cm^{-1} corresponds to the Ca-OH bond [30]. Molecular modelling [34] and far-IR spectra [35] of CSH systems also showed peaks in the same region, related to the vibrations of $Ca(OH)_2$ grains forming in the mesopores of the cementitious material. Apart for minor differences related to NR, discussed below, one can notice how the spectra from the four mortar samples, with and without fillers and NR, closely resemble each other. This brings to the conclusion that the average structure and dynamics of hydrogen within the mortars is not affected by the inclusion of rGO, MWCNT, and NR at the investigated concentrations. The same conclusion can be drawn from the spectra of filler dispersions that well reproduced that of bulk H_2O (the spectra are not shown for sake of brevity).

The two mortar systems including the NR dispersions, of which the main component is polyisoprene (PIP), manifest an additional intensity clearly visible around 200 cm^{-1} in Figure 1, likely related to the CH_3 torsion mode in PIP [36]. The signal from PIP in the two composites was isolated by subtraction of the corresponding sample prepared without natural rubber. The results are shown in Figure 2 and compared to the spectra from Adams et al. [36] available from the TOSCA INS Database [37]. Despite some noise in the resulting spectra, related to the small amount of natural rubber in the sample (about 1%wt), one can appreciate how the features from PIP in both mortar samples, with and without carbonaceous fillers, closely resemble those from bulk PIP. A slight shift in the first peak (200 cm^{-1}) is likely related to the fact that the reference spectrum was measured on a previous version of the TOSCA spectrometer (TFXA), with lower resolution at the elastic line (0 cm^{-1}) providing a larger background below 200 cm-1. Because of such background, it is difficult to infer if the clear feature at around 100 cm^{-1} was absent in bulk PIP. However, over the entire range of intermolecular vibrations, the peak positions in both mortar samples closely match those from Adams et al. [36]. Such similarities in the region of intermolecular vibrations highlight that negligible interactions take place between NR with the rest of cementitious-based hydration phases and other components of the mortar matrix.

Structural and morphological characterization

Figure 3 shows the crystalline phases present in each composite sample at the end of the hydration process. M_0 and M_1 samples show quartz as main crystalline phase (silica sand, ICCD #01-083-2465) and presented also traces of un-hydrated calcium silicate (C_3S, ICCD #01-086-0402) (see the most intense reflection at 2q = 26.63° and 29.40° respectively). Otherwise, CM_2 and CM_3 composites did not revealed any unreacted phases. In fact, besides the quartz peaks, traces of typical hydrated products such as Hydrate calcium silicate-CSH (ICCD # 00-033-0306, the main peak is tobermorite at 2q = 28.40° and the amorphous band around 30-31° [26, 27, 38]) for CM_2 and CM_3 and calcium hydroxide, CH (ICCD # ICCD # 00-033-0306, the main peak is at 2q = 36.55°) for CM_3 (reflection at 35°) were clearly detected [39]. These diffraction features confirm that the carbonaceous fillers, both MWCNTs and rGO are able to increase the hydration kinetics of the cementitious phases in the mortar, as already verified by Lin et al. [40], who observed that graphene oxide speed-up the cement hydration enhancing the assembly of the CH crystals produced during the hydration (mainly for the CM_3) process [41].

The morphological structure of mortar samples is shown in Figure 4. The utilization of the D2 and D3 aqueous dispersions significantly affected the morphological structure of mortars (Figure 4c and 4d respectively) as compared with the control sample (M_0, Figure 4a) and M_1 (produced with D1 dispersion, Figure 4b). For instance, from SEM micrographs in Figure 4a1, 4b1, 4c1, 4d1 and 4a2, 4b2, 4c2 and 4d2, the presence of a diffuse porosity [42, 43] is observed in the structure of the M_1 and CM_3 (which could be ascribed to the presence of NR latex dispersions) and CM_2 samples (which could be ascribed to a poor interaction between the carbonaceous filler with cementitious matrix), conversely M_0 composite looks like more compact. Furthermore, M_0 and M_1 highlighted the typical amorphous structure of cement-based materials whereas the hydrated products (CSH and Hydrated Aluminate-CA) were not clearly highlighted (see the SEM pictures in Figure 4a2 and 4a3) [26, 27, 44]. As also evidenced by WAXD analysis, the addition of carbonaceous fillers (D2 and D3 aqueous dispersions) promoted, speeding-up, the formation of hydrated phases, and the characteristic star-like structure of CSH was observed for CM_2 (see the SEM microstructure in Figure 4c2 and 4c3) and CM_3 (see the SEM microstructure in Figure 4d2) [26, 27]. In addition, for the composite mortars the presence of MWCNTs was clearly detected (see the inset in the Figure 4c3 and 4d3) [45]. More difficult is to detect the presence of rGO which was dispersed as nanoparticles in the matrix and get confused among the several phases present in the composite mortars. In particular, MWCNTs present in CM_3 (Figures 4d2 and 4d3) are more homogenously dispersed, mainly as single carbon nanotubes or small bundles and intertwined with the hydrated phases of the cement and some rGO platelets. On the other side, for the CM_2 sample (Figures 4c2 and 4c3) the MWCNTs appear mainly as coarse aggregates, evidencing their difficulties to homogeneously disperse in the hydrophilic environment of composite mortars. The results confirm the beneficial effect of the NR latex dispersion to endow a better distribution of the carbonaceous filler throughout the volume of hydrated cementitious phases, avoiding the formation of detrimental coarse aggregates.

Mechanical and piezoresistive characterization

To investigate piezoresistive behavior of cement-based composites, the time-dependent electrical resistance (R) variations, over 100 mechanical compression cycles for CM_2 and CM_3 samples was measured. The composites were submitted to a relatively small compressive deformation (strain < 0.6%) in order to study mechanical and piezoresistive properties in the linear elastic region (Figure 5a).

Compressive elastic modulus values (E_C) of composite mortars were calculated from compressive strain-curves of Figure 5b. E_C values of 294 ± 15 MPa and 209 ± 27 MPa were assessed for CM_2 and CM_3 systems respectively, after 5 loading/unloading cycles. Furthermore, CM_3 composite show lower value of the compressive stress (σ_C) at strain of ~ 0.6% than CM_2 composite. Hence, the introduction of the NR latex in the mortar matrix induces a decrease of E_C and σ_C values, although the filler aqueous dispersions induce a better hydration of cementitious anhydrous phases as confirmed by WAXD and SEM analysis. Finally, it is worth noting that for the composite mortar CM_2, the stress-strain curves after 5 and 60 loading/unloading compression cycles slightly differ each other, highlighting a reduction of the mechanical performances above all up to 0.2% strain which increase with the compression cycles. This difference is markedly reduced for the samples CM_3, highlighting the capability of natural rubber inclusions to improve the strain deformation of the composite mortar, avoiding the localization of internal microcracks. In fact, the NR, due to the poor bonds with cement matrix, influences the mechanical behaviour of specimens, since it contributes to weakness the interfacial transition zone [45] between the aggregated and the hydrated phases of cement and promote the formation of voids (as confirmed by SEM images in Figure 4). Turki *et al.* found a decrease of E_C and σ_C values of mortar-rubber composites as increasing the rubber content, and ascribed it to the weak interactions of the interfacial transition zone between rubber aggregates and the cementitious structures [46]. Moreover, the decrease of the compressive modulus is also associated to the intrinsic elastic properties of the NR. Indeed, Turatsinze *et al.* demonstrated that the incorporation of rubber particles in cement paste, if on the one hand reduces the compressive modulus and stress of the cement-based composites, on the other hand, it is beneficial in terms of strain and toughness capacity. The rubber material acts as crack arrester and gives rise to cementitious mortars which adsorb more of the compression energy before macrocracking localization and consequent structural collapse. Finally, they also pointed out to the beneficial effect of rubber on the reduction of cracking extent from shrinkage, which significantly contributes to the mechanical properties of composite mortars. [47] Similar results were also recently obtained by Gampanart Sukmak *et al.*, who published on the positive effect of addition of NR latex to improving the flexural strength and toughness of composite mortar through the formation of a rubber-based film which permeate the structure, whilst retarding the setting time and hydration. [48].

Piezoresistive results of Figure 6 show that CM_2 (Figure 6a) does not have a reproducible electrical trend; in fact, the electrical resistance increases with the number of loading/unloading cycles. This increase may be ascribed to both an electric polarization of fillers in the cement-based composite [49, 50] and to a modification of the MWCNTs and rGO fillers spatial distribution in the mortar matrix. Indeed, during loading/unloading compressive cycles, local cracks and slips may occur, as also confirmed by the mechanical results (see Figure 5b). The microcracks modify the spatial arrangement of carbon fillers in

the cement-based binding phase and, some carbonaceous nanoparticles, i.e. MWCNTs and rGO, irreversibly separated or disconnected from each other, due to the increased distance between the cracked surfaces, with a consequent increase of the electrical resistance. [51, 52]

On the contrary, the CM_3 (Figure 6b) composite, which has a better strain capability due to the presence of rubber phase, exhibits a regular resistance variation over loading and unloading cycles, without any performance degradation. That suggests that the mortar composite modified with rubber has a relative high reliability in strain-sensing process. As shown in Figure 6b, the electrical resistance decreases with the increasing compressive strain and increases as the compressive strain decreases, changing between the maximum and minimum values at different cycles. This behavior confirms that the carbonaceous filler densifies during compression, realizing more effective contacts which improve the electrical conductivity. When the compression load is released, the carbonaceous fillers recover their initial spatial distribution, and that brings the electrical resistance to its initial value. So the piezoresistive behavior of the composite mortars, both CM_2 and CM_3 is connected with the re-construction and de-construction of the conductive network, over loading/unloading compressive cycles. Moreover, the variation of the electrical resistance for the CM_3 composite, after a single compression cycle at ~ 0.6% strain, is higher than that of the CM_2 composite. These results suggest that the presence of the NR in the CM_3 sample generates a better spatial arrangement of the carbonaceous filler, contributing to increase the sensitivity and piezoresistive properties of the composite. Similar conclusions have been already found by Wang et al [53] for MWCNTs/polydimethylsiloxane nanocomposites with a segregated structure of the carbon filler. The sensitivity of piezoresistive material can be evaluated by the gauge factor, GF, defined as the ratio of relative resistance change ($\Delta R/R_0$) to applied strain. GF values of 0.34 and of 0.70 have been found for CM_2 and CM_3 respectively. The higher piezoresistive sensitivity of the CM_3 sample is ascribed to a more efficient de-construction and re-construction of the fillers network during compression cycles.

Finally the presence of NR coupled with the carbonaceous fillers plays a double effect in the composite mortars: i) it contributes to reducing both the compressive modulus of the sample CM_3 compared to that of the sample CM_2 and the occurring of local cracks and slips during repeated compression cycles, thus avoiding irreversible modifications in the spatial arrangement of fillers;[47] ii) it contributes to building-up a more effective conductive fillers spatial segregated arrangement within the mortar matrix, which facilitates the re-construction and de-construction of conductive percolation paths as compared with the randomly filler structure obtained in the CM_2 system without NR. The effect of segregated carbon filler structures in enhancing piezoresistive properties of polymer and natural rubber-based composites has already been investigated, [54, 55] while, as far as we know, it has never been highlighted in cement-based composites.

Hence, the presence of the NR latex, inducing better segregated structures of the rGO/MWCNTs fillers increase the sensitivity and electrical conductivity of mortar composites, indicating that the utilization of rubber-based filler composite dispersion as raw material for the preparation of composite mortars is a

valuable method in developing effective mortar-based piezoelectric sensors, which can be potentially used for developing smart buildings and infrastructures.

Conclusions

Cement-based composites with a rGO/MWCNTs well-distributed morphology were prepared by using an innovative approach consisting of assembling carbonaceous fillers onto NR latex particles with subsequent addition in the cement-based matrix. The effects of the introduction of the natural-rubber latex on distribution of carbonaceous fillers into the cement phase and on the resulting structural, morphological mechanical and piezoresistive properties of mortar-composites were thoroughly investigated. The Inelastic Neutron Scattering results highlight that the average structure and dynamics of hydrogen within the mortars are not affected by the inclusion of natural rubber, rGO, and MWCNTs at the investigated concentrations. Moreover, negligible molecular interactions take place between NR with the rest of components of the mortar matrix which do not affect the hydration processes of cement particles. X-Ray diffraction and morphological analysis show that the carbonaceous fillers speed-up the formation of hydrated phases (Hydrated Calcium Silicate, CSH) enhancing the assembly of the calcium hydroxide (CH) crystals produced during the hydration process. Furthermore, SEM analysis reveals that the introduction of the NR latex in mortar-based composite leads to a more homogeneous distribution of carbonaceous fillers throughout the volume of hydrated cementitious phases compared to the mortar-based composite obtained without NR.

Finally, the inclusion of natural rubber contributes to improving the strain deformation of the composite mortar and inducing a homogeneous fillers distribution into the mortar matrix which increases the piezo-resistive sensitivity of mortar composites compared to the system produced without rubber, which evidence the presence of MWCNTs/rGO coarse aggregates. Therefore, the obtained results suggest that the utilization of rubber-based conductive filler composite dispersion as a raw material for the preparation of mortar composites is a valuable method in developing of cement-based effective and reliable piezoresistive strain sensors.

materials

Portland cement (Type IV, Mapei Spa, Milan, Italy) [56, 57] and normalized sand (CEN-Standard Sand according to EN 196-1, grain size distribution ranging in 0.08-2.00 mm, Mapei Spa, Milan, Italy) were used in the preparation of cement-based samples. Tap water, conforming to European Standard EN 1008:2004 [58] was used to prepare mortar specimens.

Prevulcanized natural rubber latex (NR) (HMR 10, solid content: 60.5wt%) was supplied by Synthomer, UK. Reduced Graphene Oxide was produced through the chemical reduction of Graphene Oxide by ascorbic acid (AA) treatment, which was supplied by VWR Chemicals. Multi Walled Carbon Nanotubes (MWCNT) (NC 7000, diameter: 10 nm, length: 1.5 μm, density: 1.75 g/cm^3) were purchased from Nanocyl

S.A., Belgium. Cetyltrimethylammonium bromide (CTAB), as a surfactant, was obtained from Sigma Chemicals Company.

Sample preparation

Preparation of reduced Graphene Oxide (rGO)

rGO was prepared through the chemical reduction of GO assisted by ascorbic acid, accordingly to a consolidated procedure [59, 60]. In details, GO (1.65 mg/mL), obtained by graphite through a modified Hummers method [61], was dispersed in water by using an ultrasonic bath (temperature: 25°C, frequency: 40 KHz, amplitude: 100%) for 30 min. Ascorbic acid was added to the GO dispersion and the mixture was stirred at 60°C for 4h. The GO/AA weight ratio was fixed to 1:20. The obtained rGO dispersion was filtered, and the particles washed with distilled water to remove the excess of ascorbic acid.

Preparation of filler-based aqueous dispersions

rGO, MWCNTs and CTAB with a rGO/MWCNTs/CTAB weight ratio of 1:1:2 were dispersed into tap water by using an ultrasound probe (temperature: 0 °C, cycle: 0.5, amplitude: 80%) for 30 min. NR latex dispersion was added into the obtained rGO/MWCNT/CTAB dispersion and further sonicated for 30 min. In order to investigate the roles of carbonaceous fillers (mixture 1:1 wt/wt of rGO and MWCNTs) and NR on hydration mechanisms of the anhydrous cementious phases, composite samples containing only fillers and only the NR latex particles were also prepared. Therefore, for the realization of composite mortars three different filler-based aqueous dispersions, with and without rubber were prepared (see Table 1).

Table 1. Formulation of filler-based aqueous dispersions

Sample Dispersion	H_2O	NR-latex	MWCNT	rGO	CTAB
D1	84.40	15.60	-	-	-
D2	98.00	-	0.56	0.56	0.88
D3	89.38	8.90	0.48	0.48	0.76

Preparation of Cement-based Composite mortars

The composite mortars were manufactured first by mixing and dry-homogenizing suitable amount of the powders (cement and sand). Subsequently, an appropriate amount of filler-based aqueous dispersions (D1, D2 and D3) was gradually added to the dry mixture in order to be uniformly mixed (the details of the mix-design formulations are reported in Table 2). The wet mixture was then poured in a 2 x 2 x 2 cm^3 mould, and the whole system was cured in a climatic chamber (20°C and 100% RH). After 28 days, the cured samples were demoulded and put in an oven at 40 °C for 24 hours. A reference mortar produced by

using only water (H_2O) was also prepared (M_0). All the composites were then comprehensively characterized in terms of chemical, morphological and functional properties (i.e. piezoresistive properties).

Table 2. Formulations of the manufactured composite mortars

Sample	Cement (wt%)	Sand (wt%)	H_2O (wt %)	D1 (wt%)	D2 (wt%)	D3 (wt%)
M_0	22	66	12	-	-	-
M_1	22	66	-	12	-	-
CM_2	22	66	-	-	12	-
CM_3	22	66	-	-	-	12

Methods

To assess the effect of the several filler-based dispersions (including the dispersion made of pristine rubber latex) on cement hydration process, the produced cement-based composites were characterized by means of Inelastic Neutron Scattering (INS) [23, 28, 22]. In details, INS experiments were performed on the TOSCA spectrometer [23, 62] at the ISIS Neutron and Muon Source, UK. Samples were loaded in flat Al containers and measured within a closed-cycle refrigerator at the temperature of 20 K, to minimize the Debye-Waller factor [24]. The several filler dispersions (described in Table 1) were loaded in 1-mm-thick indium-sealed containers, while mortars were placed as prepared, without the need to grind the samples, with approximate thickness of 2.5 mm. Aluminum is generally used as sample container owing to its low scattering cross section for neutrons [63], thus providing a negligible self-attenuation correction [64].

Mineralogical phases evolution during hydration of cement phases were evaluated by means of XRD using a Panalytical X'Pert Pro diffractometer equipped with PixCel 1D detector (operative conditions: CuKα1/Kα2 radiation, 40 kV, 40 mA, 2Θ range from 5 to 80°, step size 0.0131° 2Θ, counting time 40s per step). The cement-based samples were finally milled before the XRD analysis.

The microstructural and morphological structure of new phases originated from cement hydration and the interactions with the filler rubber-based dispersions were evaluated by Scanning Electron Microscopy, SEM, (FEI Quanta 200 FEG scanning electron microscope-ESEM, Eindhoven, The Netherlands). The cement-based composite samples were cross-sectioned, gold sputtered, and analyzed at an accelerating voltage of 20 kV.

The experimental setup for the evaluation of the mechanical and piezoresistive properties was assembled by using a mechanical tester (Instron 5564 dynamometer) and a multimeter (Agilent 34401A

6½ Digit Multimeter) controlled by a homemade LabVIEW program. The multimeter was connected with two electrodes (a 2-probe measurement method) to the composite samples (cubic samples of 1.5cm^3), and the change in the electrical resistance of the specimen submitted out to loading and unloading cycles was continuously monitored by using a dedicated computer. A preload of 200 N was applied to ensure continuous contact of the electrodes along the entire contact surface. In details, the electrodes were realized with copper conductive tape able to glue the two opposite surfaces of the cubic sample. The electrical resistance changes were evaluated by submitting the composite samples at 100 cyclic loading/unloading, with 0.5% deformation and 0.3 mm/min actuation rate, at room temperature (22 °C).

Declarations

Acknowledgments

The work was supported by the PRIN SUSTAIN/ABLE- SimultaneoUs STructural And energetIc reNovAtion of BuiLdings through innovativE solutions. PE8LineaC-Prot. 20174RTL7W.

The authors gratefully acknowledge the financial support from Regione Lazio (IR approved by Giunta Regionale n., Grant No. G10795, August 7, 2019, published by BURL n. 69 August 27, 2019), ISIS@MACH (I), and the ISIS Neutron and Muon Source (UK) of Science and Technology Facilities Council (STFC); the financial support from the Consiglio Nazionale delle Ricerche within CNR-STFC [Grant Agreement No. 2014-2020 (N 3420)], concerning collaboration in scientific research at the ISIS Neutron and Muon Source (UK) of Science and Technology Facilities Council (STFC), is gratefully acknowledged.

The authors are grateful to Ing Vico Valassi for the support and useful discussions, and to Fabio Docimo (CNR-IPCB), Mariarosaria Marcedula Alessandra Aldi (CNR-IPCB) and Dr Svemir Rudić (ISIS) for their technical support.

Author contributions

L. Verdolotti, C. Santillo, B. Liguori, G. Rollo and G. Lama carried out the experiments, chemico-physical and piezoresistive characterizations and data elaboration with the support of M. Lavorgna. G. Romanelli, E. Preziosi, R. Senesi and C. Andreani carried out the INS experiments and the corresponding data elaboration. Verdolotti L, C. Santillo and M. Lavorgna wrote the manuscript with support from the other authors. M. Lavorgna and M. Di Prisco helped supervise the project. M. Lavorgna, M. Di Prisco and C. Andreani conceived the original idea.

Competing interests

All the authors declare no competing interests.

Data availability

The datasets generated during and/or analysed during the current study are available from the corresponding authors on reasonable request.

References

1. Dimov, D. *et al*. Ultrahigh performance Nanoengineered Graphene-concrete composites for multifunctional applications. *Funct. Mater.***28**, 1-12 (2018).
2. Chuah, S., Pan, Z., Sanjayan, J. G., Wang, C. M., Duan, W. H. Nano reinforced cement and concrete composites and new perspective from graphene oxide. *Build. Mater.***73**, 113-124 (2014).
3. Sun, S. *et al*. Nano Graphite Platelets-Enabled Piezoresistive Cementitious Composites for Structural Health Monitoring. *Build. Mater.***136**, 314-328 (2017).
4. Zheng, Q., Han, B., & Ou, J. NanoComposites for structural health monitoring. In *Nanotechnology in Eco-efficient Construction* (Second Edition) 227-259 (Woodhead Publishing, 2019).
5. Reddy, P. N., Kavyateja, B. V., & Jindal, B. B. Structural health monitoring methods, dispersion of fibers, micro and macro structural properties, sensing, and mechanical properties of self-sensing concrete-A review. *Structural Concrete* (2020).
6. Ghosh, S., Harish, S., Rocky, K. A., Ohtaki, M., Saha, B. B. Graphene enhanced thermoelectric properties of cement based composites for building energy harvesting. *Energy Build*. **202**, 109419 (2019).
7. Hongyu, S., Binmeng, C., Bo, L., Shengwen, T., Zongjin, L. Influence of dispersants on the properties of CNTs reinforced cement-based materials. *Build. Mater.***131**, 186–194, (2017).
8. Zhang, L., *et al*. Effect of characteristics of assembly unit of CNT/NCB composite fillers on properties of smart cement-based materials. *Part A Appl. Sci. Manuf.***109**, 303–320 (2018).
9. Zhan, M., Pan, G., Zhou, F., Mi, R., Shah, S. P. In situ-grown carbon nanotubes enhanced cement-based materials with multifunctionality. *Concr. Compos.***108**, 103518 (2020)
10. Han, B. *et al.* Electrostatic self-assembled carbon nanotube/nano carbon black composite fillers reinforced cement-based materials with multifunctionality. *Part A Appl. Sci. Manuf.***79**, 103–115 (2015).
11. Konsta-Gdoutos, M.S., Danoglidis, P.A., Falara, M.G., Nitodas, S.E. Fresh and mechanical properties, and strain sensing of nanomodified cement mortars: the effects of MWCNT aspect ratio, density and functionalization, *Concr. Compos*. **82**, 137–151 (2017).
12. Han, J., Pan, J., Cai, J., Li X. A review on carbon-based self-sensing cementitious composites. *Build. Mater.***265**, 120764 (2020).
13. Parveen, S., Rana, S., Fangueiro, R. A review on nanomaterial dispersion, microstructure, and mechanical properties of carbon nanotube and nanofiber reinforced cementitious composites, *Nanomater.***2013**, 1–19 (2013).
14. Ur Rehman, S. K., Kumarova, S., Memon, S. A., Javed, M. F., Jameel, M. A Review of Microscale, Rheological, Mechanical, Thermoelectrical and Piezoresistive Properties of Graphene Based Cement

Composite. *Nanomaterials***10**, 2076 (2020).

15. Hossain, M.M., Karim, R., Hasan, M., Hossain, M.K., Zain, M.F.M. Durability of mortar and concrete made up of pozzolans as a partial replacement of cement: A review. *Build. Mater.***116**, 128-140 (2016).
16. Xu, Y. *et al*. A holistic review of cement composites reinforced with graphene oxide, review *Build. Mater.* **171**, 291-302 (2018).
17. Bai, S., Jiang, L., Xu, N., Jin, M., Jiang, S. Enhancement of mechanical and electrical properties of graphene/cement composite due to improved dispersion of graphene by addition of silica fume. *Build. Mater.***164**, 433-441(2018).
18. Zhan, Y., Lavorgna, M., Buonocore, G.G., Xia, H. Enhancing electrical conductivity of rubber composites by constructing interconnected network of self-assembled graphene with latex mixing. ***Mater. Chem.* 22**, 10464-10468 (2012).
19. Salzano De Luna, M. *et al*. Nanocomposite polymeric materials with 3D graphene-based architectures: from design strategies to tailored properties and potential applications. *Polym. Sci.***89**, 213-249 (2019).
20. Toghroli, A. *et al*. A review on pavement porous concrete using recycled waste materials. *Struct. Syst.***22**, 433-440 (2018).
21. Letelier, V., Tarela, E., Muñoz, P., Moriconi, G. Assessment of the mechanical properties of a concrete made by reusing both: Brewery spent diatomite and recycled aggregates. *Build. Mater.***114**, 492-498 (2016).
22. Parker, S. F. *et al*. TOSCA: a world class inelastic neutron spectrometer. *B Condens. Matter*, **241-243**, 154–156 (1997).
23. Fernandez-Alonso, F., Price, D.L. Neutron Scattering – Fundamentals, Academic Press, New York, (2013).
24. Mitchell, P. C. H. Vibrational spectroscopy with neutrons: with applications in chemistry, biology, materials science and catalysis, World Scientific, **3** (2005).
25. Ricci, M. A., Nardone, M., Fontana, A., Andreani, C., Hahn, W. Light and neutron scattering studies of the OH stretching band in liquid and supercritical water. *Chem. Phys.***108** (2), 450-454 (1998).
26. Senesi, R., *et al.* The quantum nature of the OH stretching mode in ice and water probed by neutron scattering experiments. *Chem. Phys.***139** (7), 074504 (2013).
27. Senesi, R., Romanelli, G., Adams, M. A., Andreani C. Temperature dependence of the zero point kinetic energy in ice and water above room temperature. *Phys.***427**, 111-116 (2013).
28. Squires G. L. Introduction to the theory of thermal neutron scattering. Courier Corporation, (1996).
29. Festa G., *et al.* Old burned bones tell us about past cultures. *Eur.* **31**, 18-21 (2019).
30. Thomas, J. J., Chen, J., Jennings, H. M., Neumann, D. A. Ca-OH Bonding in the C-S-H Gel Phase of Tricalcium Silicate and White Portland Cement Pastes Measured by Inelastic Neutron Scattering. *Chem. Mater.***15**, 3813-3817 (2003).

31. Bordallo, H. N., Aldridge, L. P., Desmedt, A. Water Dynamics in Hardened Ordinary Portland Cement Paste or Concrete: From Quasielastic Neutron Scattering. *Phys. Chem.***110**, 17966-17976 (2006).
32. Peterson, V. K., Brown, C. M., Livingston, R. A. Quasielastic and inelastic neutron scattering study of the hydration of monoclinic and triclinic tricalcium silicate. *Phys.***326**, 381-389 (2006).
33. Faraone, A., Fratini, E., Baglioni, P., Chen, S. H. Quasielastic and inelastic neutron scattering on hydrated calcium silicate pastes. *Chem. Phys.***121** (7), 3212 (2004).
34. Pellenq, R. J.-M., *et al*. A realistic molecular model of cement hydrates. *Natl. Acad. Sci.***106**, 16102–16107 (2009).
35. Yu, P., Kirkpatrick, R. J., Poe. B., McMillan, P. F., Cong, X. Structure of Calcium Silicate Hydrate (C-S-H): Near-, Mid-, and Far-Infrared Spectroscopy. *Am. Ceram. Soc*. **82**, 742–48 (1999).
36. Adams, M.A., Gabrys, B. J., Zajac, W. M., Peiffer, D. G. High-Resolution Incoherent Inelastic Neutron Scattering Spectra of Polyisobutylene and Polyisoprene. *Macromolecules* **38**, 160-166 (2005).
37. ISIS INS Database, 2020,https://www.isis.stfc.ac.uk/Pages/INS-database.aspx.
38. Omotoso, O.E., Ivey, D. G., Mikula, R. Hexavalent chromium in tricalcium silicate Part I Quantitative X-ray diffraction analysis of crystalline hydration products. *Mat. Sci.***33**, 507-513 (1998).
39. Xu, G., Du, S., He, J., Shi, X. The role of admixed graphene oxide in a cement hydration system. *Carbon***148**, 141-150 (2019).
40. Lin, C., Wei, W., Hu, Y.H. Catalytic behavior of graphene oxide for cement hydration process. *Phys. Chem. Solids*, **89**, 128-133 (2016).
41. Lia, W. *et al.* Effects of graphene oxide on early-age hydration and electrical resistivity of Portland cement paste. *Build. Mater.***136**, 506-514 (2017).
42. De Luca Bossa, F., *et al*. Greener Nanocomposite Polyurethane Foam Based on Sustainable Polyol and Natural Fillers: Investigation of Chemico-Physical and Mechanical Properties. *Materials***13**, 211 (2020).
43. Stanzione, M., *et al*. Tuning of polyurethane foam mechanical and thermal properties using ball-milled cellulose. *Polym.* **231**, 115772 (2020).
44. Tambara Júnior, L. U. D., Cheriaf, M., Rocha, J. C. Development of Alkaline-Activated Self-Leveling Hybrid Mortar Ash-Based Composites. *Materials***11**, 1829 (2018).
45. Prokopski, G, Halbiniak, J. Interfacial transition zone in cementitious materials. *Concr. Res*. **30**, 579–83 (2000).
46. Turki, M., Bretagne, E., Rouis, M.J., Quéneudec, M. Microstructure, physical and mechanical properties of mortar–rubber aggregates mixtures. *Build. Mater.***23**, 2715-2722 (2009).
47. Turatsinze, A., Bonnet, S., Granju, J.-L. Mechanical characterisation of cement-based mortar incorporating rubber aggregates from recycled worn tyres. *Environ.***40**, 221–226 (2005).
48. Sukmak, G., *et al*. Physical and mechanical properties of natural rubber modified cement paste, *Build. Mater.***244**, 118319 (2020).

49. Rao, R., Sindu, B.S., Sasmal, S. Synthesis, design and piezo-resistive characteristics of cementitious smart nanocomposites with different types of functionalized MWCNTs under long cyclic loading. *Concr. Compos.***108**, 103517 (2020).
50. Wen, S., Chung, D.D.L. Partial replacement of carbon fiber by carbon black in multifunctional cement–matrix composites. *Carbon* **45**, 505–513 (2007).
51. Tao, J., Wang, X., Wang, Z., Zeng, Q. Graphene nanoplatelets as an effective additive to tune the microstructures and piezoresistive properties of cement-based composites. *Build. Mater.***209**, 665–678 (2019).
52. Yoo, D. Y., You, I., Lee, S. J. Electrical and piezoresistive sensing capacities of cement paste with multi-walled carbon nanotubes. Arch. Civ. Mech. Eng. **18**, 371–384 (2018).
53. Wang, M., *et al*. Enhanced electrical conductivity and piezoresistive sensing in multi-wall carbon nanotubes/polydimethylsiloxane nanocomposites via the construction of a self-segregated structure. *Nanoscale***9**, 11017 (2017).
54. Zhai, W., *et al*. Segregated conductive polymer composite with synergistically electrical and mechanical properties. *Part A Appl. Sci. Manuf.***105**, 68-77 (2018).
55. Lin, Y., *et al*. Graphene–Elastomer Composites with Segregated Nanostructured Network for Liquid and Strain Sensing Application. *ACS Appl. Mater. Interfaces***8**, 24143–24151 (2016).
56. Verdolotti, L., Di Maio, E., Lavorgna, M., Iannace, S. Hydration-induced reinforcement of rigid polyurethane–cement foams: Mechanical and functional properties. *Mater. Sci.***47**, 6948–6957 (2012).
57. Verdolotti, L., Di Maio, E., Forte, G., Lavorgna, M., Iannace, S. Hydration-induced reinforcement of polyurethane-cement foams: Solvent resistance and mechanical properties. *Mat. Sci.***45**, 3388–3391 (2010).
58. Mixing Water for Concrete-Specification for Sampling, Testing and Assessing the Suitability of Water, Including Water Recovered from Processes in the Concrete Industry, as Mixing Water for Concrete; BSI: London, UK, **10**, 1008 (2002).
59. Zhang, J., *et al.* Reduction of graphene oxide via L-ascorbic acid. *Commun.***46**, 1112–1114 (2010).
60. Fernandez-Merino, M. J. Vitamin C Is an Ideal Substitute for Hydrazine in the Reduction of Graphene Oxide Suspensions. *Phys. Chem. C*. **114**, 6426–6432 (2010).
61. Zhan, Y., Lavorgna, M., Buonocore, G.G., Xia, H. Enhancing electrical conductivity of rubber composites by constructing interconnected network of self-assembled graphene with latex mixing. *Mater. Chem.***22** (21), 10464–10468 (2012).
62. Rudic, S., *et al*. TOSCA international beamline review, STFC technical report (2013).
63. Sears, V. F. Neutron scattering lengths and cross sections. *Neutron News***3**, 26-37 (1992).
64. Scatigno, C. *et al*. A Python Algorithm to Analyze Inelastic Neutron Scattering Spectra Based on the y-Scale Formalism. *Chem. Theor. Comp.***16**, 7671-7680 (2020).

Figures

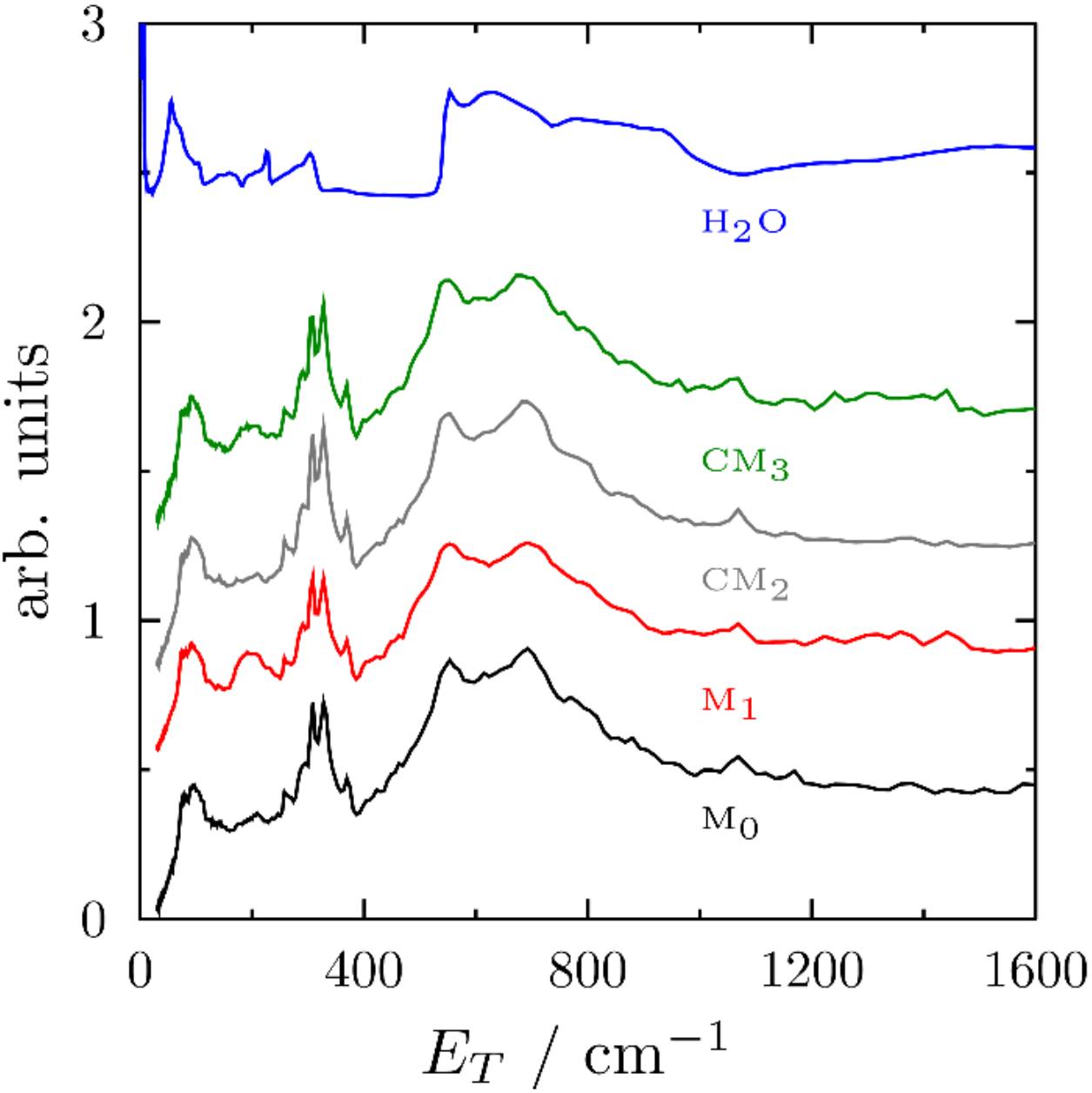

Figure 1

Experimental INS spectra of M0 (black); M1 (red); CM2 (grey); CM3 (green); and bulk H2O (blue). Spectra have been scaled and shifted vertically to ease visualization and comparison.

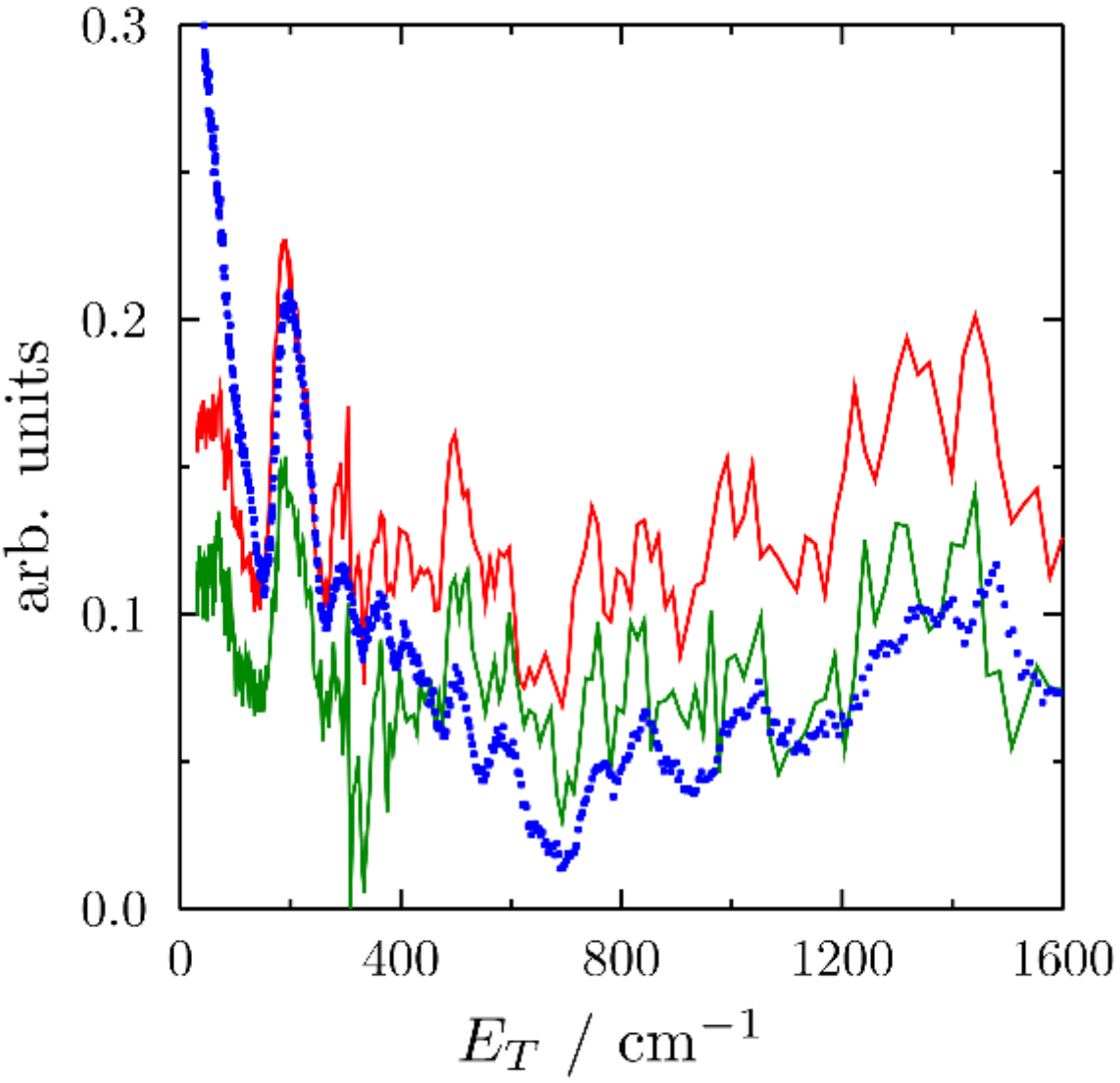

Figure 2

Experimental INS spectra of natural rubber from M1 (red); CM2 (green); and its bulk phase (blue) from Ref. (36, 37).

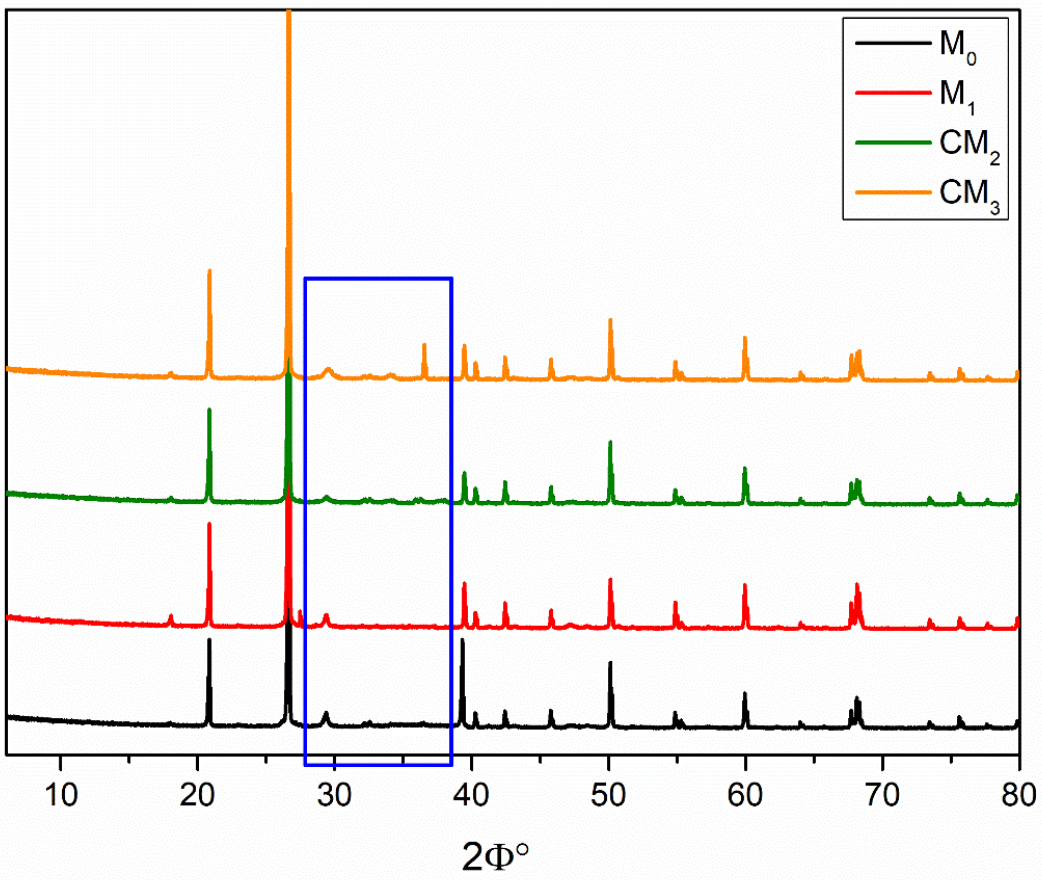

Figure 3

X-ray Diffraction spectra of composite mortar samples after the hydration process

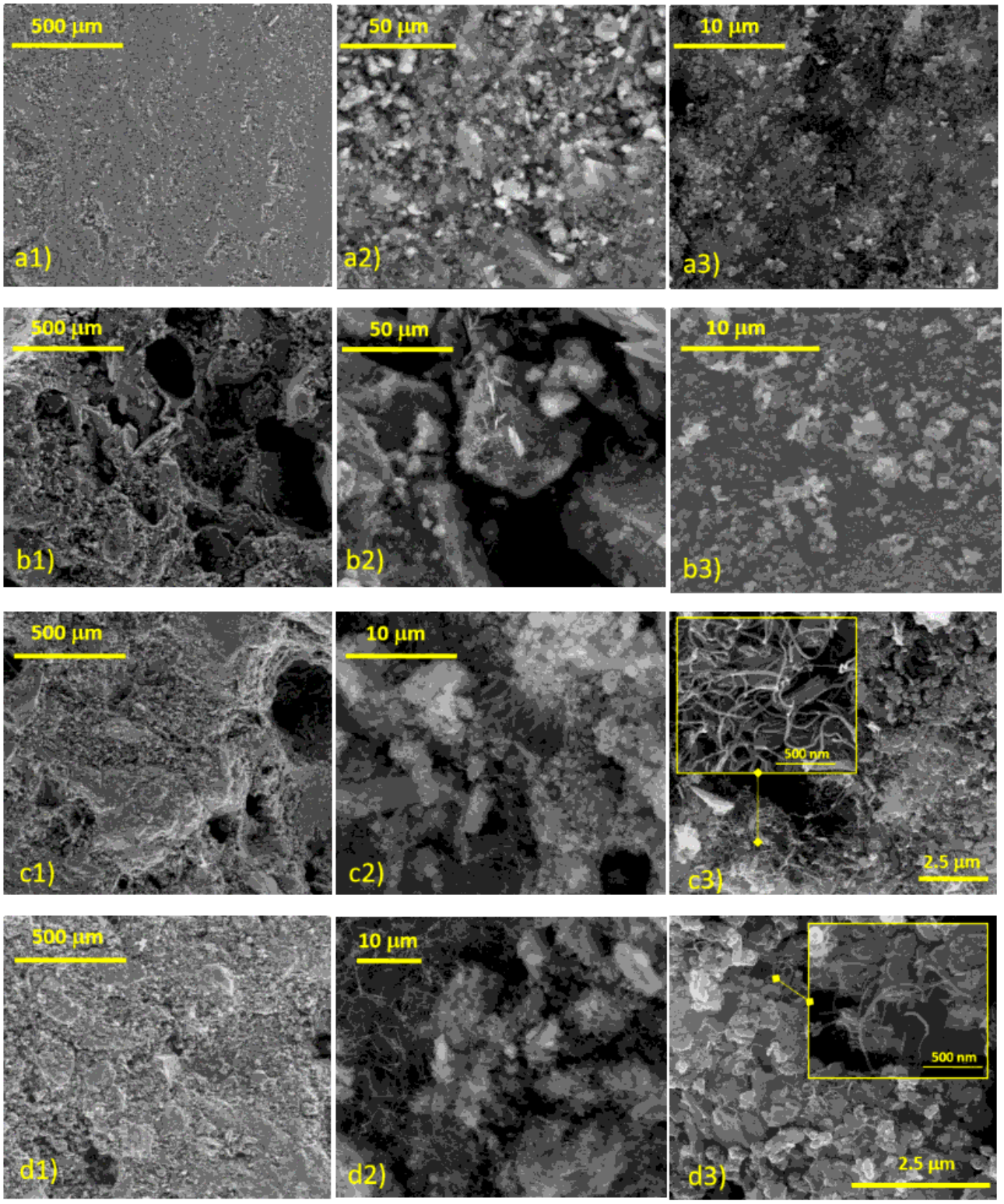

Figure 4

SEM images at different magnifications of a) M0, b) M1, c) CM2, and d) CM3

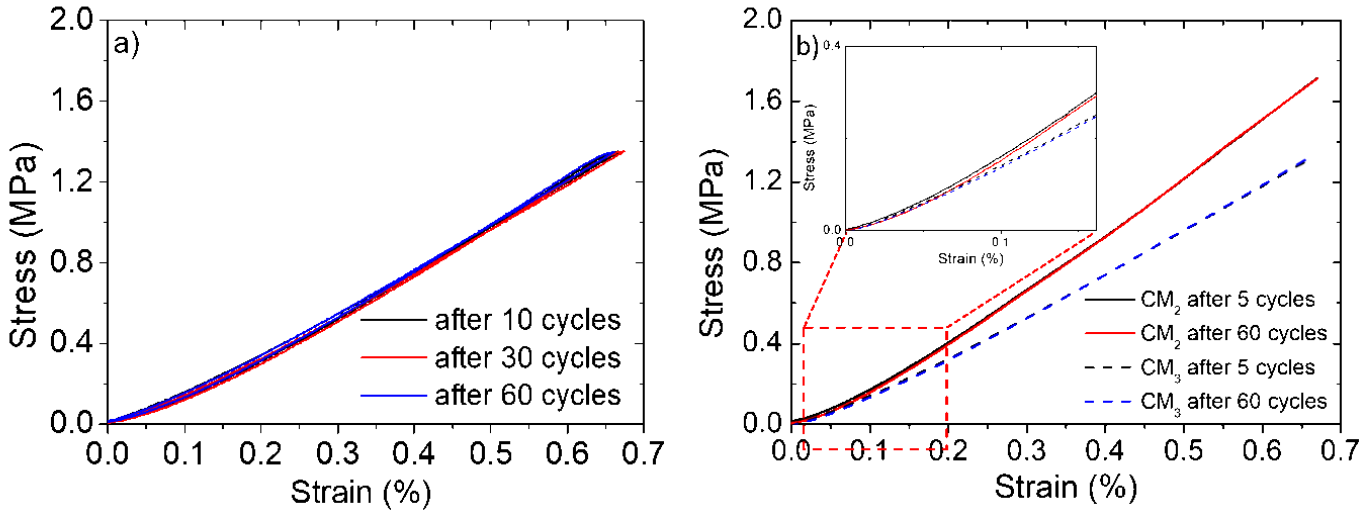

Figure 5

a) Compressive stress-strain curves after 10, 30 and 60 cycles for CM3 b) Compressive stress-strain curves of CM2 and CM3 samples after 5 and 60 loading/unloading cycles.

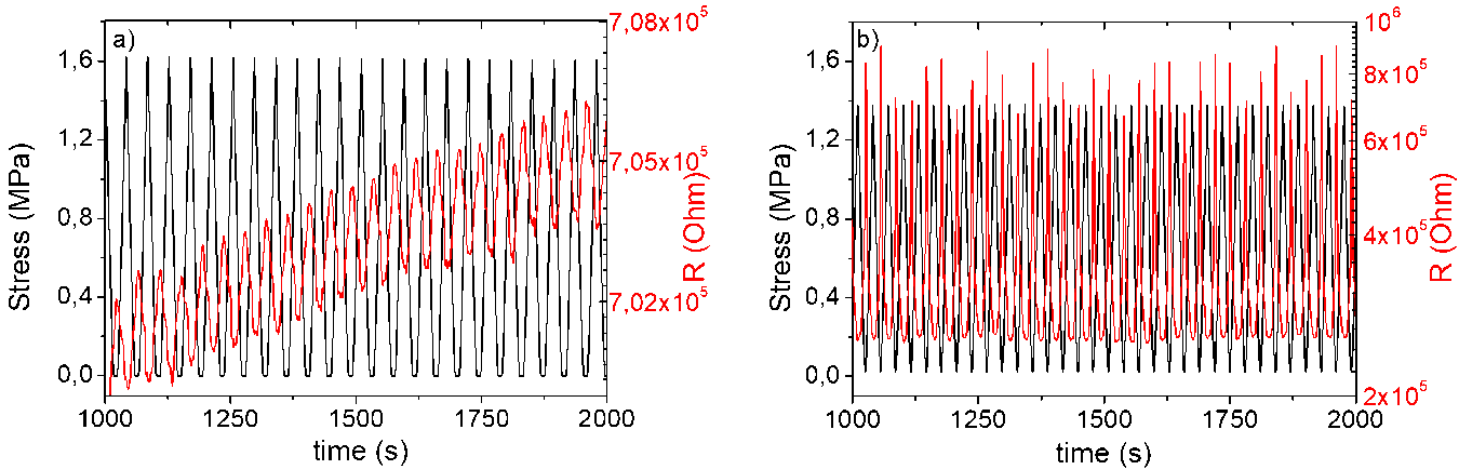

Figure 6

Piezoresistive behaviour, in terms of variation of compression stress and electrical resistance for the systems CM2 a) and CM3 b).